Ab Initio Studies on Cyanoacetylene Oligomers: Rings and Chains versus Stacked Clusters

Alfred Karpfen

Institut für Theoretische Chemie und Strahlenchemie, Universität Wien, A-1090 Wien, Währingerstrasse 17, Austria

Received: June 9, 1998

The structures and the vibrational spectra of cyanoacetylene clusters were investigated with the aid of ab initio Møller−Plesset second-order calculations using large polarized basis sets. In addition to ring- and chainlike structures, stacked non-hydrogen-bonded configurations, in which chainlike oligomers are oriented in an antiparallel fashion, were investigated. Particular emphasis has been given to a more thorough investigation of selected sections of the energy surface of the cyanoacetylene dimer, including the search for parallel and antiparallel stacked structures and for π-type hydrogen-bonded configurations. This search revealed that apart from the linear dimer which corresponds to the energetically most stable dimer, a second minimum corresponding to a C_{2h} stacked antiparallel dimer is quite close in energy, whereas π-type hydrogen-bonded configurations and parallel but slipped stacked arrangements are barely bound. The relatively high stability of the antiparallel stacked dimer has the consequence that larger stacked clusters, e.g., tetramers and hexamers, are likely to be of similar stability as the corresponding cyclic oligomers or are even the dominant species and that both, stacked and cyclic configurations, are significantly more stable than linear clusters from the tetramers on. Most of the experimentally observed infrared-active C−H stretching frequencies could be successfully assigned to particular oligomers.

Introduction

Recently, high-resolution infrared spectra of the cyanoacetylene dimer[1] and of cyanoacetylene clusters[2] in the gas phase were reported. In these investigations, the C−H stretching region, most sensitive to subtle changes in the hydrogen-bonding conditions, was thoroughly scanned. In close analogy to the well-investigated case of hydrogen cyanide in the gas phase,[3−11] the spectra of the smaller clusters were interpreted in terms of linear dimers and trimers and of a cyclic trimer. In the case of the larger clusters,[2] several peaks, all of them originating from nonpolar species, were observed. However, because of insufficient rotational resolution, the assignment of these peaks to particular oligomer structures was not possible. For the tetramer several conceivable nonpolar configurations were suggested by Yang et al.,[2] among them a pinwheel structure stabilized by π-type hydrogen bonding, a cyclic structure with conventional C−H- - -N hydrogen bonds, and a configuration built from two stacked and eventually slipped antiparallel dimers.

So far, quantum chemical calculations on cyanoacetylene clusters are very few in number. Apart from some earlier ab initio self-consistent field (SCF) geometry optimizations on the linear dimer[12,13] and a very recent Møller−Plesset second-order (MP2) calculation of a few geometries of the antiparallel dimer,[14] the only previous theoretical work in which the structure and vibrational spectra of the cyanoacetylene dimer and of larger clusters have been treated was presented by the present author.[15] In ref 15, extensive ab initio calculations were performed, applying SCF, MP2, and density-functional theory (DFT) methods. In that investigation, the search for the most stable cyanoacetylene cluster configurations were restricted to linear and cyclic arrangements up to the size of hexamers and the discussion of calculated vibrational properties dealt exclusively with the C−H stretching region.

In this work, an attempt is made to extend the investigations of ref 15, to evaluate the relative importance of oligomer structures other than the consecutively hydrogen-bonded cyclic or linear configurations, and to present improved calculations on the structure of these complexes, together with a more comprehensive description of their vibrational spectra. To this end and after a discussion of the necessary requirements on the description of the monomer properties, a more thorough investigation of the potential energy surface of the cyanoacetylene dimer is presented as an important first step. Evidently, given the size of the monomer and considering the computational demands on the reliability of such calculations, a reasonably complete scan of the four-dimensional (4D) intermolecular energy surface is currently, by far, out of reach. Hence, only a few selected 2D cuts through the dimer energy surface, which appeared as promising candidates for energetically attractive configurations, have been considered. All of these 2D cuts were done with a fixed angular orientation of structurally frozen monomers. Nonplanar arrangements have been excluded from this investigation. In the next step, the properties of the two stable dimer configurations, a linear $C_{\infty v}$ and an antiparallel C_{2h} structure, are discussed in some detail.

In the following sections, the structures and the vibrational spectra of the larger clusters are described, with the main aims (i) to provide a more detailed interpretation of the gas-phase infrared spectra reported by Yang et al.,[2] (ii) to allow for a better understanding of the probable cluster configurations in the transition region from small clusters to solidlike arrangements, and (iii) to predict spectroscopically observable features that have so far not been investigated experimentally.

Method of Calculation

All quantum chemical calculations were performed with the Gaussian 94 suite of programs.[16] Because of the nature of the

10.1021/jp982558n CCC: $15.00
Published on Web 10/27/1998

TABLE 1: Computed MP2 Total Energies (E), Rotational Constants (B_e), Equilibrium Structures, Dipole Moments (μ), and Parallel ($\alpha_{||}$) and Perpendicular ($\alpha_\perp$) Polarizabilities of the Cyanoacetylene Monomer

	basis set				
	I[a]	II[a]	III[a]	IV	V
E [hartree][b]	−0.086325	−0.159231	−0.204597	−0.206143	−0.242725
B_e [GHz]	4.454	4.524	4.499	4.498	4.510
r(H−C) [Å]	1.0640	1.0629	1.0652	1.0652	1.0628
r(C≡C [Å]	1.2236	1.2116	1.2159	1.2162	1.2162
r(C−C) [Å]	1.3770	1.3701	1.3728	1.3729	1.3710
r(C≡N) [Å]	1.1875	1.1752	1.1789	1.1789	1.1759
μ [Debye]	3.712	3.723	3.778	3.769	3.783
$\alpha_{||}$ [Å^3]	8.902	9.484	9.901	9.975	9.939
$\alpha_\perp$ [Å^3]	1.980	2.469	3.258	3.816	3.679

[a] Structures already reported in ref 15. [b] 169 hartrees to be added to each entry.

problem, the majority of the calculations were performed with the MP2 method.[17] However, where appropriate, comparison is also made to the results of SCF and B3LYP approaches. The latter is one of the recent DFT variants, in which Becke's hybrid exchange B3[18,19] and the Lee, Yang, Parr nonlocal correlation functional (LYP)[20,21] are used.

Most of the basis sets applied are identical to those already used in ref 15 and in earlier calculations on hydrogen cyanide clusters.[22−24] Basis set I is the 6-31G(d,p) basis.[25,26] Basis set II is the 10s6p/6s Huzinaga[27,28] basis set contracted to 6s4p/4s and augmented by a set of d functions on nitrogen (0.95) and carbon (1.0) and a set of p-functions on hydrogen (0.75). Basis set III is the 11s7p/6s Huzinaga[27,28] basis set contracted to 7s5p/4s and augmented by two sets of d functions on nitrogen (0.95, 0.3) and carbon (1.0, 0.3) and a set of p functions on hydrogen (0.75). Basis set IV consists of basis set III plus additional flat s, p, and d functions on nitrogen (0.04/0.03/0.1) and carbon (0.03/0.02/0.1) and flat s and 2p functions on hydrogen (0.03/0.2, 0.05), thus, overall a contracted 8s6p3d/7s3p basis. Basis set V is the 6-311++G(3df,3dp) basis.[26,29,30] Basis set IV was used for monomer calculations and for a 2D scan of the antiparallel dimer, basis set V for monomer calculations only.

In case of the 2D scans performed for several configurations of the cyanoacetylene dimer, points of regular meshes with step sizes of 0.5 and 0.25 Å for Δz and Δx, respectively, have been computed where z corresponds to the molecular axis of one fixed cyanoacetylene molecule, and the second molecule is translated in Δz and Δx directions. At the MP2-optimized geometries of the various clusters, the influence of the basis set superposition error (BSSE) has been evaluated with the aid of the conventional counterpoise procedure,[31] including the effect of monomer geometry relaxation.

Results and Discussion

A. Monomer. The calculated total energies (E), the rotational constants (B_e), the optimized geometries, the dipole moments (μ), and the polarizabilities parallel, $\alpha_{||}$, and perpendicular, $\alpha_\perp$, to the molecular axis are compiled in Table 1. Probably the most reliable structure of the cyanoacetylene monomer published so far is the one reported by Botschwina et al.[32] Their values of 1.0624, 1.2058, 1.3764, and 1.1605 Å for r(H−C), r(C≡C), r(C−C), and r(C≡N), respectively, as obtained from large-scale coupled electron-pair approximation (CEPA) calculations in combination with fits to experimental rotational constants (4.549 GHz[33]), are reasonably close to the data of Table 1. SCF- and B3LYP-optimized structures, as obtained with basis sets I−III, had already been reported in ref 15. Further theoretical structures are also available from recent MP2,[34,35] coupled cluster,[36] and DFT[37] calculations and may also be compared to the data of Table 1.

Whereas the computed dipole moments do not depend too sensitively on the size of the basis set and are all very close to the experimental value of 3.724 D,[38] a correct description of the computed polarizabilities, in particular, of the polarizability $\alpha_\perp$, perpendicular to the molecular axis requires the addition of sufficiently flat, i.e., small exponent basis functions. Our best values for $\alpha_{||}$ and $\alpha_\perp$ around 9.98 and 3.82 Å^3, respectively, as obtained with basis set IV, may be compared to those reported by Fowler and Diercksen,[39] who obtained 9.715 and 3.722 Å^3 at the MBPT2 level applying specifically designed polarized basis sets. Interestingly and in agreement with the findings of Fowler and Diercksen, for each of the basis sets chosen our computed SCF and also the B3LYP polarizabilities are very close to the corresponding MP2 numbers. Whereas $\alpha_{||}$, as obtained with basis set I (6-31G(d,p)), is only 10% lower than the basis set IV value, the basis set I value for $\alpha_\perp$ is only one-half the basis set IV result. With basis sets II and III, this anisotropy ratio is progressively improved.

The accurate description of monomer dipole moments *and* polarizabilities *and* the polarizability anisotropy is a necessary ingredient when probing different sections of the intermolecular energy surface, for which either electrostatic effects, e.g., in hydrogen-bonded configurations, or dispersion effects, e.g., in parallel or antiparallel dimers, give rise to the dominating contributions to the intermolecular interaction energy.

The computed harmonic vibrational frequencies and infrared intensities of the cyanoacetylene monomer are collected in Table 2 and shall mainly serve as a reference for the cluster vibrational frequencies to be discussed later. With several of the basis sets applied, some of the MP2-computed harmonic bending frequencies are already distinctly lower than the experimental fundamentals.[40,41] This behavior is well-known and can be traced back to the lack of f functions in the atomic basis sets,[42] the inclusion of which would make cluster calculations prohibitively expensive.

B. Dimer. Selected Sections of the Dimer Energy Surface. The most stable structure, i.e., the global minimum on the intermolecular energy surface of the cyanoacetylene dimer, is probably the linear C−H- - -N hydrogen-bonded configuration. Other conceivable alternatives for stable dimer configurations are (i) a π-type hydrogen bond formed between the C−H group of the hydrogen-bond donor and one of the two triple bonds of the hydrogen-bond acceptor, (ii) antiparallel stacked dimers, and (iii) parallel stacked (slipped) dimers. These four configurations are shown schematically in Figure 1. Applying basis sets II and III, 2D energy surfaces have been scanned for configurations b−d of Figure 1. All of these scans have been performed without correcting for BSSE.

Let us first discuss the π-type hydrogen-bond configuration. A contour map for displacing the second cyanoacetylene

TABLE 2: Computed MP2 Harmonic Vibrational Frequencies and Infrared Intensities of the Cyanoacetylene Monomer[a]

	basis set					
	I	II	III	IV	V	expl[b]
	Stretching Frequencies					
ω_1 (C−H)	3531 (81)	3503 (78)	3460 (83)	3460 (81)	3471 (85)	3327
ω_2 (C≡N)	2246 (8.5)	2239 (7.0)	2212 (6.7)	2210 (6.2)	2223 (6.8)	2274
ω_3 (C≡C)	2052 (4.6)	2052 (2.3)	2029 (2.8)	2027 (2.4)	2034 (2.6)	2079
ω_4 (C−C)	891 (0.38)	885 (0.49)	876 (0.35)	875 (0.37)	882 (0.31)	885
	Bending Frequencies					
ω_5 (CCH)	610 (91)	629 (91)	622 (90)	597 (83)	643 (79)	663
ω_6 (CCN)	502 (2.2)	377 (1.4)	428 (3.4)	399 (1.9)	505 (5.0)	499
ω_7 (CCC)	237 (2.2)	181 (0.56)	206 (0.52)	197 (0.62)	226 (0.56)	222

[a] Frequencies in cm^{-1}, infrared intensities in parentheses in km mol^{-1}. [b] Fundamentals as reported in refs 39 and 40.

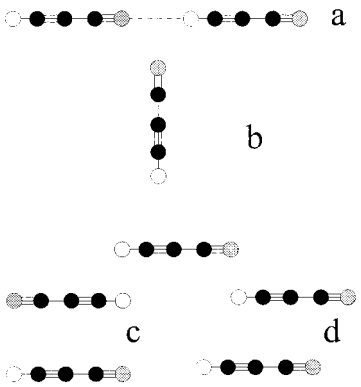

Figure 1. Schematic structures of cyanoacetylene dimer configurations: linear hydrogen-bonded dimer (a), π-type hydrogen-bonded dimer (b), antiparallel stacked dimer (c), and parallel stacked dimer (d).

molecule in parallel and perpendicular directions relative to the first is shown in Figure 2. These data have been obtained with basis set III at the MP2 level. At a position where one might expect an optimal arrangement for a π-type hydrogen bond to the C≡C triple bond, i.e, around $\Delta z = 1.7$ Å and $\Delta x \approx 2.6$ Å, only a very flat potential region is observed with, at best, an extremely shallow minimum. Moreover, the interaction energy is very small and barely attractive. Even a C−H - - - N≡C hydrogen bond with a 90° H···N≡C angle is much more stable than the π-type hydrogen bond to the C≡C triple bond. Thus, the π-type hydrogen bond is not a good candidate for a stable dimer structure and is at least more than 3 kcal mol^{-1} less stable than the linear C−H- - -N≡C hydrogen bond.

A contour plot for the parallel stacked configuration is shown in Figure 3. As with the π-type hydrogen bond discussed before, only a shallow, weakly attractive minimum with a binding energy of about −1 kcal mol^{-1} can be observed. Thus, both the π-type hydrogen bond and the parallel stacked structure cannot compete with the stability of the linear dimer.

In Figure 4, contour plots for the case of the antiparallel stacked dimer are shown, as obtained with basis sets III and IV. This time, a distinct, strongly attractive minimum is found in the vicinity of $\Delta z = 0$ and $\Delta x \approx 3.5$ Å with a binding energy close to −4 kcal mol^{-1}. The shallow regions of the energy

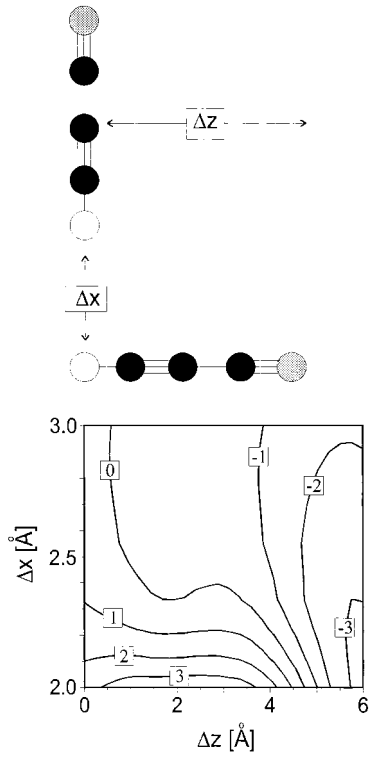

Figure 2. Contour plot for *x*,*z*-translations of a cyanoacetylene monomer in a perpendicular orientation to a fixed cyanoacetylene molecule. Energy values obtained from MP2 calculations applying basis set III. Contour labels in kcal mol^{-1} relative to twice the monomer energy. The upper picture indicates $\Delta z = 0$.

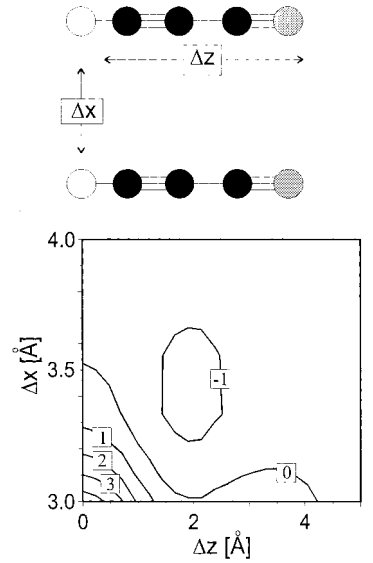

Figure 3. Contour plot for x,z-translations of a cyanoacetylene monomer in a parallel orientation to a fixed cyanoacetylene molecule. Energy values obtained from MP2 calculations applying basis set III. Contour labels in kcal mol^{-1} relative to twice the monomer energy. The upper picture indicates $\Delta z = 0$.

surface to the right and left of this minimum correspond to slipped stacked antiparallel arrangements. However, no deep minima appear in these cases. Hence, from these limited scans, it would appear that the only reasonable alternative to the linear dimer is the antiparallel stacked dimer in a nonslipped C_{2h} configuration with two 90° distorted (this time the C−H- - -N bond angle is about 90°) hydrogen bonds. Consequently, full geometry optimization and vibrational analyses have been carried out for the stacked antiparallel dimer, and they are

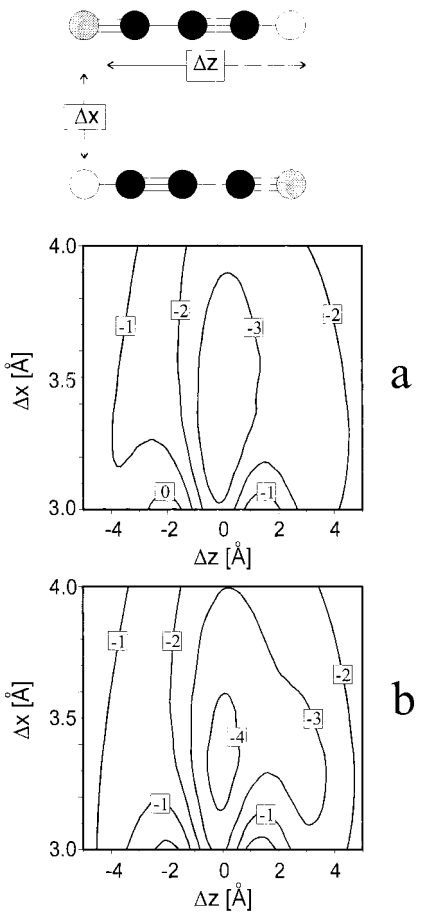

Figure 4. Contour plots for *x*,*z*-translations of a cyanoacetylene monomer in antiparallel orientation to a fixed cyanoacetylene molecule. Energy values obtained from MP2 calculations applying basis set III (a) and basis set IV (b). Contour labels in kcal mol^{-1} relative to twice the monomer energy. The upper picture indicates $\Delta z = 0$.

TABLE 3: Computed MP2 Equilibrium Structures of the Linear $C_{\infty v}$ Cyanoacetylene Dimer (Å)[a]

	basis set		
	I	II	III
r(H−C)	1.0645	1.0632	1.0656
r(C≡C)	1.2235	1.2118	1.2159
r(C−C)	1.3754	1.3687	1.3712
r(C≡N)	1.1869	1.1740	1.1776
r(N- - -H)	2.2433	2.2837	2.2532
r(H−C)	1.0694	1.0680	1.0710
r(C≡C)	1.2249	1.2132	1.2175
r(C−C)	1.3762	1.3695	1.3720
r(C≡N)	1.1878	1.1753	1.1792

[a] Dimer structure assumed as in Figure 1a with the non-hydrogen-bonded H−C group at the left end. All values from ref 15.

compared to the corresponding results for the linear dimer in the following.

Linear Dimer and Antiparallel Stacked Dimer. The optimized structural parameters for the linear $C_{\infty v}$ dimer, as obtained with basis sets I−III applying SCF, B3LYP, and MP2 methods, were already reported in Table 4 of ref 15. Calculations in the vicinity of the minimum geometry of the linear dimer could not be performed with basis set IV. The shorter (by about 1 Å) intermolecular contact in the linear hydrogen-bonded structure, as compared to the antiparallel dimer configuration together with the very flat s, p, and d basis functions, resulted in severe near-linear dependence problems. Hence, in Table 3, only the MP2 results obtained with basis sets I−III are repeated in order to make the paper self-contained. The optimized structural parameters of the parallel stacked C_{2h} dimer obtained with basis sets I−III and with SCF, B3LYP, and MP2 methods are compiled in Table 4.

For all basis sets used, the MP2-optimized intermolecular distance of the linear dimer is rather close (to within 0.02 Å) to the experimental value of 2.266 Å.[1] Inspecting the computed structural parameters for the antiparallel stacked configuration, the following trends can be observed. The optimized distances (*r*(H- - -N) in the 90° distorted hydrogen bond and *r*(C−C′), the distance between the central carbon atoms of the two monomers) between the two molecules are much larger when computed within the SCF approach and are with about 3.9 Å for *r*(H- - -N) and 4.0 Å for *r*(C−C′), far outside the sum of the the van der Waals radii, clearly a consequence of the lack of dispersion interaction. The B3LYP results are within about 3.8 Å for *r*(H- - -N) and 3.9 Å for *r*(C−C′), not very different from the SCF answer, and are also significantly larger than one would expect from standard van der Waals radii. The MP2 results, on the other hand, predict much shorter intermolecular distances in the vicinity of 3.2 Å for *r*(H- - -N) and 3.4 Å for *r*(C−C′). The variation of the computed intermolecular distances obtained within a given method, but with different basis sets, are only modest. Judging from a structural point of view, even the MP2/6-31G(d,p) result (basis set I) appears tolerable. This finding is important for the following since the MP2 geometry optimizations for the larger stacked clusters were affordable only with basis set I. Subsequent vibrational analysis revealed that in the case of the antiparallel stacked dimer, irrespective of the basis set applied, all MP2 structures are minima. SCF and B3LYP structures obtained with basis set I are also minima, whereas with the other basis sets, first-order saddle points are obtained, however, with exceedingly small imaginary frequencies (about 8i and 20i for SCF and B3LYP, respectively).

The MP2 stabilization energies for both types of dimers and the corresponding BSSE-corrected values are collected in Table 5. The BSSE corrections were evaluated with monomers structurally distorted as in the complexes. The stabilization energies and the zero-point energy (ZPE) corrected stabilization energies (SCF, B3LYP, and MP2) are shown in Table 6. Analyzing first the BSSE-corrected energies, one can observe that use of the counterpoise BSSE correction for basis sets I and II does not lead to acceptable results. Whereas in the case of the linear minimum, the BSSE correction does indeed lead to more uniform interaction energies close to −4 kcal mol^{-1} and, thus, appears to achieve an improved description, it leads to erroneous results for the antiparallel stacked structure with basis sets I and II. The BSSE correction is larger in the case of the antiparallel dimer, a consequence of the larger molecular overlap. Together with the already underestimated interaction energy, due to the too small perpendicular polarizability, $\alpha_\perp$, the BSSE-corrected interaction energy is further reduced by more than 1 kcal mol^{-1} relative to the stabilization energy of the linear structure. With the larger basis set III, the BSSE corrections are much smaller for both configurations. The BSSE-corrected energy difference between the two structures amounts to about 0.5 kcal mol^{-1} only. Since with basis set III $\alpha_\perp$ is still somewhat underestimated, one might expect that the true energy difference between the two structures is actually even smaller.

The performance of the SCF, B3LYP, and MP2 approaches for the relative energies of linear and antiparallel stacked configurations can be seen in Table 6 and parallels the behavior just discussed for the intermolecular distances. SCF and B3LYP lead to somewhat lower interaction energies compared to the

TABLE 4: Computed MP2 Equilibrium Structures of the Stacked Antiparallel C_{2h} Cyanoacetylene Dimer[a]

	method								
	SCF	B3LYP	MP2	SCF	B3LYP	MP2	SCF	B3LYP	MP2
	basis set								
	I	I	I	II	II	II	III	III	III
r(H−C)	1.0585	1.0673	1.0649	1.0571	1.0646	1.0635	1.0563	1.0641	1.0661
r(C≡C)	1.1856	1.2101	1.2243	1.1780	1.2004	1.2126	1.1785	1.2007	1.2170
r(C−C)	1.3907	1.3723	1.3757	1.3865	1.3684	1.3689	1.3881	1.3690	1.3712
r(C≡N)	1.1365	1.1667	1.1878	1.1277	1.1560	1.1754	1.1288	1.1566	1.1794
r(N- - -H′)	3.7391	3.5426	3.2800	3.9488	3.8299	3.2843	3.9334	3.7810	3.2222
r(C−C′)[b]	3.8219	3.6368	3.4041	4.0292	3.9236	3.4609	4.0098	3.8728	3.3747
∠HCC	179.3	178.8	178.6	179.5	179.3	179.8	179.5	179.3	179.3
∠CCC	179.0	179.0	178.7	179.0	178.8	176.9	179.0	178.7	177.7
∠CCN	178.7	178.5	177.8	178.8	178.5	176.7	178.8	178.6	177.2
∠CNH′	91.6	91.3	92.0	92.0	92.4	92.4	91.1	91.5	91.8
∠NH′C′	90.9	91.9	92.2	90.3	90.4	92.7	91.1	91.3	93.0

[a] Distances are given in angstroms and bond angles in degrees. Dimer structure assumed as in Figure 1c. [b] Distance between the central carbon atoms of the two monomers.

TABLE 5: Computed MP2 Stabilization Energies (ΔE) and BSSE-Corrected Stabilization Energies (ΔE(BSSE)) for Linear $C_{\infty v}$ and Stacked Antiparallel C_{2h} Cyanoacetylene Dimers (kcal mol^{-1})

	basis set		
	I	II	III
	Linear		
ΔE	−4.92	−4.31	−4.34
BSSE	0.88	0.37	0.17
ΔE(BSSE)	−4.04	−3.94	−4.17
	Antiparallel		
ΔE	−3.65	−3.79	−4.02
BSSE	1.57	1.58	0.38
ΔE(BSSE)	−2.20	−2.21	−3.64

TABLE 6: Computed Stabilization Energies (ΔE) and ZPE-Corrected Stabilization Energies (ΔE(ZPE)) for Linear $C_{\infty v}$ and Stacked Antiparallel C_{2h} Cyanoacetylene Dimers (kcal mol^{-1})

		basis set		
	method	I	II	III
	Linear			
	SCF			
ΔE		−3.97	−3.68	−3.54
ΔE(ZPE)		−3.41	−3.18	−3.06
	B3LYP			
ΔE		−4.59	−3.97	−3.77
ΔE(ZPE)		−3.87	−3.37	−3.22
	MP2			
ΔE		−4.92	−4.31	−4.34
ΔE(ZPE)		−4.12	−3.81	−3.80
ΔE(BSSE + ZPE)		−3.24	−3.44	−3.63
	Antiparallel			
	SCF			
ΔE		−1.87	−1.34	−1.38
ΔE(ZPE)		−1.64	−1.19	−1.21
	B3LYP			
ΔE		−1.81	−1.14	−1.16
ΔE(ZPE)		−1.54	−0.98	−0.99
	MP2			
ΔE		−3.65	−3.79	−4.02
ΔE(ZPE)		−3.34	−3.53	−3.70
ΔE(BSSE + ZPE)		−1.77	−1.95	−3.32

MP2 numbers in the case of the linear configuration. This is in line with the behavior in other hydrogen-bonded dimers, where electrostatic and induction effects dominate. However, a radically different picture is observed for the antiparallel stacked structure. There, a substantial part of the intermolecular interaction energy is due to dispersion contributions which, by the very definition, cannot be modeled within the framework of the SCF (Hartree−Fock) approximation. Hence, a factor of ca. 3 is observed between SCF and MP2 interaction energies. As expected, the B3LYP approach behaves just as the SCF model does, in agreement with previous observations[43,44] that current DFT methods do not yield acceptable descriptions of the dispersion interaction. In view of this behavior, BSSE corrections for SCF and B3LYP calculations have been dispensed with. With basis set III, the BSSE- and ZPE-corrected interaction energy for the linear dimer is only 0.3 kcal mol^{-1} below that of the antiparallel stacked dimer.

Summarizing the structural and energetic data obtained so far from our limited potential surface scans and geometry optimizations, we obtain the picture of a stable linear dimer and of a stable antiparallel stacked dimer. Because of the basis-set problems discussed above, it is at present uncertain which of the two is actually more stable. The best value for the energy difference (MP2, basis set III, BSSE and ZPE corrected) amounts to −0.3 kcal mol^{-1} in favor of the linear dimer. From the experimental side, only the existence of the linear dimer has been established.[1,2] The antiparallel stacked dimer has so far not been detected.

Computed vibrational spectra of the linear and the antiparallel dimers obtained with basis sets I−III and with the MP2 approach are compiled in Tables 7 and 8. In all cases, all frequencies are real and, hence, both structures formally constitute minima on the energy surface. From the experimental side, only the two C−H stretching frequencies of the linear dimer have been measured. Kerstel et al.[1] reported frequency shifts relative to the C−H stretching frequency of the cyanoacetylene monomer of −3 and −66 cm^{-1} for the *free* and *hydrogen-bonded* C−H stretch, respectively. The computed values for these shifts of −2 to −4 cm^{-1} for the *free* and −67 to −78 cm^{-1} for the *hydrogen-bonded* C−H stretch, which were already reported in ref 15, agree nicely with that assignment. For the hitherto unobserved antiparallel stacked dimer, the computed C−H stretching frequency shifts range from −4 to −7 cm^{-1} and is very close to and slightly below the *free* C−H stretch of the linear dimer and also of the linear trimer. Hence, their experimental detection might, indeed, be difficult.

It is, therefore, tempting to look for other features in the computed frequency spectra which might eventually allow one to discern more easily between the two conformers. The best candidate for that purpose is probably the CCH bending frequency. In the case of the linear dimer, frequency shifts of about +90 and +7 cm^{-1} (basis sets II and III) and about +159

TABLE 7: Computed MP2 Harmonic Vibrational Frequencies, Frequency Shifts Relative to the Monomer, and Infrared Intensities of the Linear $C_{\infty v}$ Cyanoacetylene Dimer[a]

	basis set		
	I	II	III
	Intramolecular Stretching Frequencies		
ω_1 (C−H)	3527 (*−4*) [86]	3501 (*−2*) [84]	3456 (*−4*) [88]
ω_2 (C−H)	3459 (*−72*) [487]	3436 (*−67*) [427]	3382 (*−78*) [475]
ω_3 (C≡N)	2252 (*6*) [22]	2245 (*6*) [21]	2218 (*6*) [22]
ω_4 (C≡N)	2242 (*−4*) [42]	2235 (*−4*) [38]	2207 (*−5*) [41]
ω_5 (C≡C)	2058 (*6*) [3]	2057 (*5*) [1]	2035 (*6*) [2]
ω_6 (C≡C)	2046 (*−6*) [29]	2046 (*−6*) [20]	2022 (*−7*) [24]
ω_7 (C−C)	901 (*10*) [0]	893 (*8*) [0]	884 (*8*) [0]
ω_8 (C−C)	892 (*1*) [1]	886 (*1*) [0]	877 (*1*) [1]
	Intramolecular Bending Frequencies		
ω_9 (CCH)	769 (*159*) [75]	719 (*90*) [75]	712 (*90*) [68]
ω_{10} (CCH)	618 (*8*) [92]	637 (*8*) [88]	629 (*7*) [85]
ω_{11} (CCN)	514 (*12*) [1]	376 (*−1*) [2]	431 (*3*) [7]
ω_{12} (CCN)	500 (*−2*) [2]	372 (*−5*) [5]	430 (*2*) [3]
ω_{13} (CCC)	249 (*12*) [2]	187 (*6*) [0]	217 (*11*) [0]
ω_{14} (CCC)	236 (*−1*) [3]	178 (*−3*) [1]	206 (*0*) [1]
	Intermolecular Stretching Frequency		
ω_{15} (CH- - -N)	87 [2]	79 [2]	81 [2]
	Intermolecular Bending Frequencies		
ω_{16}	67 [12]	58 [13]	57 [13]
ω_{17}	16 [1]	13 [1]	13 [1]

[a] Frequencies and shifts relative to the monomer (in italics and in parentheses) in cm^{-1}, infrared intensities in square brackets in km mol^{-1}.

TABLE 8: Computed MP2 Harmonic Vibrational Frequencies, Frequency Shifts Relative to the Monomer, and Infrared Intensities of the Antiparallel C_{2h} Cyanoacetylene Dimer[a]

	basis set		
	I	II	III
	Intramolecular Stretching Frequencies		
ω_1 (C−H) a_g	3523 (*−7*)	3497 (*−6*)	3451 (*−4*)
ω_2 (C−H) $b_{u'}$	3523 (*−7*) [160]	3497 (*−7*) [154]	3451 (*−4*) [162]
ω_3 (C≡N) b_u	2245 (*−1*) [24]	2238 (*−1*) [23]	2209 (*−3*) [24]
ω_4 (C≡N) a_g	2243 (*−3*)	2235 (*−4*)	2207 (*−5*)
ω_5 (C≡C) b_u	2050 (*−2*) [10]	2049 (*−3*) [6]	2025 (*−4*) [8]
ω_6 (C≡C) a_g	2049 (*−3*)	2048 (*−4*)	2024 (*−5*)
ω_7 (C−C) a_g	893 (*2*)	888 (*3*)	879 (*3*)
ω_8 (C−C) b_u	893 (*2*) [0]	888 (*3*) [0]	878 (*2*) [0]
	Intramolecular Bending Frequencies		
ω_9 (CCH) a_u	629 (*19*) [87]	636 (*7*) [81]	637 (*13*) [77]
ω_{10} (CCH) b_g	628 (*18*)	635 (*6*)	636 (*12*)
ω_{11} (CCH) a_g	602 (*2*)	637 (*8*)	623 (*1*)
ω_{12} (CCH) b_u	601 (*1*) [107]	637 (*8*) [97]	624 (*2*) [98]
ω_{13} (CCN) b_g	511 (*9*)	356 (*−21*)	425 (*−3*)
ω_{14} (CCN) a_u	511 (*9*) [0]	359 (*−18*) [2]	426 (*−2*) [4]
ω_{15} (CCN) a_g	495 (*−7*)	382 (*5*)	425 (*−3*)
ω_{16} (CCN) b_u	495 (*−7*) [4]	378 (*1*) [4]	427 (*−1*) [3]
ω_{17} (CCC) b_g	241 (*4*)	166 (*−15*)	207 (*1*)
ω_{18} (CCC) a_u	238 (*1*) [2]	176 (*−5*) [0]	205 (*−1*) [1]
ω_{19} (CCC) b_u	237 (*0*) [2]	184 (*3*) [1]	209 (*3*) [1]
ω_{20} (CCC) a_g	232 (*−5*)	190 (*9*)	207 (*1*)
	Intermolecular Stretching Frequency		
ω_{21} a_g	81	80	84
	Intermolecular Bending Frequencies		
ω_{22} b_u	53 [16]	59 [16]	61 [17]
ω_{23} a_g	50	48	53
ω_{24} a_u	35 [11]	23 [10]	33 [10]

[a] Frequencies and shifts relative to the monomer (in italics and in parentheses) in cm^{-1}, infrared intensities in square brackets in km mol^{-1}.

and +8 (basis set I) relative to the monomer are predicted for *hydrogen-bonded* and *free* CCH bending modes, respectively.

TABLE 9: Computed MP2 Equilibrium Structures of the Linear $C_{\infty v}$ Cyanoacetylene Trimer (Å)[a]

	basis set		
	I	II	III
r(H−C)	1.0646	1.0633	1.0657
r(C≡C)	1.2235	1.2118	1.2159
r(C−C)	1.3752	1.3685	1.3710
r(C≡N)	1.1858	1.1739	1.1775
r(N- - -H)	2.2176	2.2565	2.2261
r(H−C)	1.0704	1.0689	1.0720
r(C≡C)	1.2251	1.2133	1.2176
r(C−C)	1.3742	1.3677	1.3702
r(C≡N)	1.1861	1.1742	1.1779
r(N- - -H)	2.2202	2.2602	2.2266
r(H−C)	1.0702	1.0687	1.0719
r(C≡C)	1.2251	1.2134	1.2177
r(C−C)	1.3760	1.3694	1.3719
r(C≡N)	1.1879	1.1753	1.1792

[a] Trimer structure assumed as commencing with the non-hydrogen-bonded H−C group at the left end.

The difference between the basis set I results and the larger basis-set results appears to be systematic and probably points to the need for scaling down the basis set I CCH bending mode shifts. In the case of the antiparallel stacked dimer, shifts of +13 and +2 (basis set III), +7 and +8 (basis set II), and +19 and +1 (basis set I) are predicted for the two infrared-active CCH bends. Thus, the shift patterns are very different for the CCH bending modes of these two dimers. Although for the other vibrational bands there are also some differences between the two structures, it appears that they are hardly sufficiently significant.

For the linear dimer, MP2 dipole moments of 8.77, 8.59, and 8.76 D were obtained with basis set I−III, respectively, corresponding to dipole moment enhancements of 15−18% relative to the vectorially added monomer dipole moments. An experimental value has not yet been reported.

C. Trimer. In case of the trimers, it appears that there are only two structures which can reasonably be related to the experimental data: the linear $C_{\infty v}$ trimer as a polar cluster and the cyclic C_{3h} trimer as a nonpolar cluster. Further alternatives, like a trimer consisting of alternating antiparallel dimers, trimers consisting of a preformed linear dimer with the third monomer in some kind of antiparallel stacked configuration, or trimers with bifurcated hydrogen bonds, have been excluded from this investigation since they would not give rise to nonpolar structures. That does not necessarily imply that minima of these types do not exist. On the contrary, most probably, there are local minima of that type but it is expected that these cannot compete in stability with the linear and cyclic forms.

The computed equilibrium structures of the linear and cyclic trimers and the shifts of the C−H stretching frequencies were already discussed in some detail in ref 15. Compared to that work, additional MP2 optimizations applying basis set III and computationally already exceedingly heavy MP2 frequency calculations on the linear trimer applying basis set II have been carried out. The optimized structural parameters of the linear and cyclic trimers are reported in Tables 9 and 10, and the computed harmonic frequencies are compiled in Tables 11 and 12.

In the linear trimer, the two intermolecular distances happen to have very similar values. The same applies to the two C−H bond distances in the C−H- - -N hydrogen bonds. As a consequence of this structural feature, the two C−H stretching frequencies originating from the hydrogen-bonded C−H groups are also very close to each other. Therefore, the system behaves like a pair of two nearly equal and weakly coupled oscillators

TABLE 10: Computed MP2 Equilibrium Structures of the Cyclic C_{3h} Cyanoacetylene Trimer[a]

	basis set		
	I	II	III
r(H−C)	1.0670	1.0656	1.0683
r(C≡C)	1.2248	1.2129	1.2173
r(C−C)	1.3746	1.3680	1.3703
r(C≡N)	1.1876	1.1753	1.1791
r(N- - -H)	2.4594	2.4748	2.4451
∠(H−C≡C)	177.0	177.8	177.2
∠(C≡C−C)	179.0	178.6	178.9
∠(C−C≡N)	178.6	178.2	178.5
∠(C≡N- - -H)	119.8	119.0	120.0
∠(N- - -H−C)	125.6	126.5	125.5

[a] Distances are given in angstroms and angles in degrees.

TABLE 11: Computed MP2 Harmonic Vibrational Frequencies, Frequency Shifts Relative to the Monomer, and Infrared Intensities of the Linear $C_{\infty v}$ Cyanoacetylene Trimer[a]

	basis set	
	I	II
Intramolecular Stretching Frequencies		
ω_1 (C−H)	3526 (*−5*) [88]	3500 (*−3*) [85]
ω_2 (C−H)	3449 (*−82*) [23]	3427 (*−76*) [23]
ω_3 (C−H)	3459 (*−92*) [1108]	3423 (*−80*) [963]
ω_4 (C≡N)	2253 (*7*) [30]	2246 (*7*) [25]
ω_5 (C≡N)	2248 (*2*) [74]	2241 (*2*) [72]
ω_6 (C≡N)	2241 (*−5*) [48]	2234 (*−5*) [48]
ω_7 (C≡C)	2059 (*7*) [1]	2058 (6) [1]
ω_8 (C≡C)	2052 (*0*) [23]	2051 (*−1*) [15]
ω_9 (C≡C)	2045 (*−7*) [48]	2045 (*5*) [32]
ω_{10} (C−C)	907 (*16*) [3]	897 (*12*) [2]
ω_{11} (C−C)	898 (*7*) [1]	891 (*6*) [1]
ω_{12} (C−C)	893 (*2*) [0]	886 (*1*) [0]
Intramolecular Bending Frequencies		
ω_{13} (CCH)	785 (*175*) [55]	730 (*100*) [77]
ω_{14} (CCH)	781 (*171*) [91]	726 (*94*) [68]
ω_{15} (CCH)	620 (*10*) [93]	638 (*9*) [87]
ω_{16} (CCN)	514 (*12*) [2]	377 (*0*) [2]
ω_{17} (CCN)	507 (*5*) [3]	372 (*−5*) [0]
ω_{18} (CCN)	501 (*−1*) [0]	371 (*−6*) [11]
ω_{19} (CCC)	253 (*16*) [0]	188 (*7*) [0]
ω_{20} (CCC)	246 (*9*) [3]	183 (*2*) [0]
ω_{21} (CCC)	236 (*−1*) [4]	176 (*−5*) [0]
Intermolecular Stretching Frequency		
ω_{22} (CH- - -N)	113 [0]	101 [0]
ω_{23} (CH- - -N)	63 [2]	57 [2]
Intermolecular Bending Frequencies		
ω_{24}	81 [18]	69 [19]
ω_{25}	58 [0]	49 [0]
ω_{26}	20 [4]	16 [4]
ω_{27}	7 [0]	6 [0]

[a] Frequencies and shifts relative to the monomer (in italics and in parentheses) in cm^{-1}, infrared intensities in square brackets in km mol^{-1}.

with the in-phase combination taking all the infrared intensity, whereas the out-of-phase combination has an almost vanishing intensity (lower by a factor of about 50) and will, hence, be hardly detectable. The very same pattern has already been encountered in the case of the linear hydrogen cyanide trimer.[5−8,15,22−24] In the cyclic trimer, the intermolecular distance (about 2.46 Å) is much longer than that in the dimer (2.26 Å). Hence, the red shift of the C−H stretches is much smaller (about 33 cm^{-1}), again paralleling the $(HCN)_3$ case. Fairly clear distinctions between cyclic and linear trimer are also to be expected in the region of the CCH bending motions. The linear trimer gives rise to two strongly blue-shifted bands

TABLE 12: Computed MP2 Harmonic Vibrational Frequencies, Frequency Shifts Relative to the Monomer, and Infrared Intensities of the Cyclic C_{3h} Cyanoacetylene Trimer As Obtained with Basis Set I[a]

intramolecular stretching frequencies		intramolecular bending frequencies	
ω_1 (C−H) e′	3498 (*−33*) [389]	ω_9 (CCH) a″	679 (*69*) [118]
ω_2 (C−H) a′	3496 (*−35*)	ω_{10} (CCH) e″	678 (*68*)
ω_3 (C≡N) e′	2245 (*−1*) [93]	ω_{11} (CCH) a′	643 (*33*)
ω_4 (C≡N) a′	2244 (*−2*)	ω_{12} (CCH) e′	647 (*37*) [296]
ω_5 (C≡C) e′	2050 (*−2*) [17]	ω_{13} (CCN) a″	514 (*12*) [2]
ω_6 (C≡C) a′	2049 (*−3*)	ω_{14} (CCN) a′	513 (*11*)
ω_7 (C−C) a′	899 (*8*)	ω_{15} (CCN) e″	512 (*10*)
ω_8 (C−C) e′	896 (*5*) [0]	ω_{16} (CCN) e′	506 (*4*) [2]
		ω_{17} (CCC) a′	248 (*11*)
		ω_{18} (CCC) e′	246 (*9*) [2]
		ω_{19} (CCC) e″	246 (*9*)
		ω_{20} (CCC) a″	240 (*3*) [2]
intermolecular stretching frequency		intermolecular bending frequencies	
ω_{21} e′	121 [32]	ω_{23} a″	57 [15]
ω_{22} a′	86	ω_{24} a′	50
		ω_{25} e″	34
		ω_{26} e′	23 [7]

[a] Frequencies and shifts relative to the monomer (in italics and in parentheses) in cm^{-1}, infrared intensities in square brackets in km mol^{-1}.

TABLE 13: Computed MP2 Stabilization Energies (ΔE), BSSE-Corrected Stabilization Energies (ΔE(BSSE)), and ZPE-Corrected Stabilization Energies (ΔE(ZPE)) for Linear $C_{\infty v}$ and Cyclic C_{3h} Cyanoacetylene Trimers (kcal mol^{-1})

	basis set		
	I	II	III
	Linear		
ΔE	−10.48	−9.18	−9.29
BSSE	1.80	0.77	0.30
ΔE(BSSE)	−8.68	−8.41	−8.99
ZPE	1.64	1.00	1.00[a]
ΔE(ZPE)	−8.84	−8.18	−8.29
ΔE(BSSE + ZPE)	−7.04	−7.41	−7.99
	Cyclic		
ΔE	−10.53	−9.52	−9.91
BSSE	2.56	1.78	0.52
ΔE(BSSE)	−7.97	−7.74	−9.39
ZPE	1.24	0.76[b]	0.76[b]
ΔE(ZPE)	−9.29	−8.76	−9.15
ΔE(BSSE + ZPE)	−6.73	−6.98	-8.63

[a] ZPE correction taken from basis set II results. [b] ZPE corrections taken from basis set I results and scaled by 1/1.64 as extracted from the basis set trends in the linear trimer.

with computed shifts of about 171 and 175 cm^{-1} (basis set I) and about 94 and 100 cm^{-1} (basis set II). The corresponding shifts in the cyclic trimer amount to 37 and 69 cm^{-1} (basis set I) only, a consequence of the much weaker hydrogen-bonding characteristics. As with the dimers, the remaining parts of the trimer spectra are probably not too helpful when it comes to discriminate between the two alternatives.

The stabilization energies of the trimers, the BSSE- and ZPE-corrected stabilization energies are shown in Table 13. Discussing first the uncorrected interaction energies, we observe that upon increasing the size of the basis set, the cyclic configuration gains stability relative to the linear configuration. Whereas with basis set I, both trimers are about equally stable, the cyclic structure is preferred by about −0.6 kcal mol^{-1} with basis set III. As with the dimers, caution is necessary when trying to

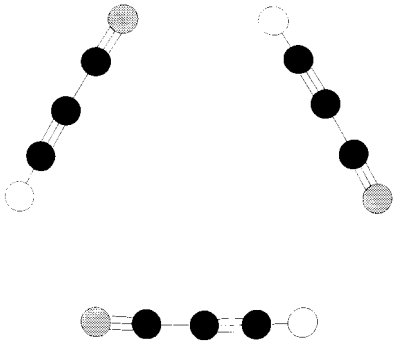

Figure 5. Structure of the cyclic cyanoacetylene trimer.

correct for the BSSE. Application of the counterpoise correction with the smaller basis sets tends to strongly prefer the linear structure. With basis set III, the BSSE correction is again considerably smaller and the BSSE-corrected interaction energies show a -0.4 kcal mol^{-1} preference for the cyclic structure.

The ZPE correction, on the other hand, is larger in the linear trimer, and hence, the ZPE correction tends to favor the cyclic structures. Overall, application of both corrections results in a slight extra stabilization of the cyclic trimer with basis set III, in addition to the preference for the cyclic structure already at the level of the uncorrected energies. Again, the trends in the stabilization energy corrections, as obtained with basis set I, are caused by the poor description of the polarizability anisotropy with basis set I and by the artificial destabilization when applying the BSSE corrections, in combination with too small basis sets, to two structures with significantly different molecular overlaps.

For the linear trimers, MP2 dipole moments of 13.88, 13.69, and 13.99 D were calculated. That corresponds to nonadditive dipole moment enhancements of about 2.52−2.74 D relative to monomers. The experimental value for the dipole moment of the linear trimer of about 11.4 D[2] is significantly smaller. This discrepancy must be caused by the fact that the experimental value corresponds to a dynamic structure vibrationally averaged over the very soft intermolecular bending degrees of freedom.

D. Tetramer. Four different tetramer structure types have been considered in this work: (i) the linear tetramer, $C_{\infty v}$, (ii) a configuration built from two linear dimers in an antiparallel stacked arrangement, C_{2h}, (iii) the pinwheel structure, C_{4h}, suggested by Yang et al.,[2] which is an arrangement with four π-type hydrogen bonds, and (iv) the cyclic tetramer, C_{4h}, with consecutive C−H- - -N hydrogen bonding. The latter three structures are depicted in Figure 6. In case of the tetramers, MP2 structure optimizations were affordable only with basis sets I and II and vibrational frequency calculations only with basis set I. The optimized structures of the tetramers are reported in Table 14. Since, as with the smaller clusters discussed so far, most of the frequency shifts related to intramolecular degrees of freedom are again small, we shall only discuss the optimized structures, the energetics, and the shifts of the C−H stretching and CCH bending frequencies.

The computed optimized structural parameters of the four tetramers are shown in Table 14. The interaction energies and the BSSE- and the ZPE-corrected interaction energies are collected in Table 15. The computed vibrational frequencies in the C−H-stretching and CCH-bending regions, the infrared intensities, and the shifts to the corresponding monomer modes are reported in Table 16.

The structures of the antiparallel stacked tetramer (see Figure 6a) and the pinwheel (see Figure 6b) are of particular interest.

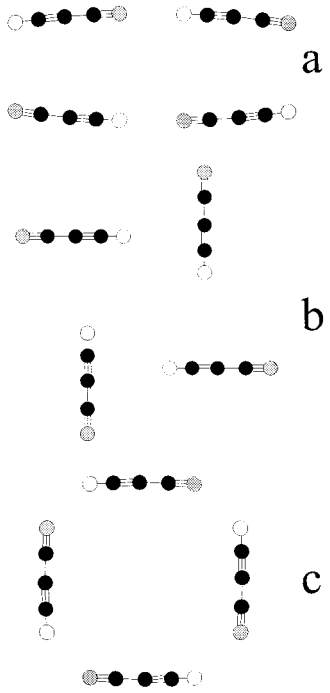

Figure 6. Structures of cyanoacetylene tetramers: antiparallel arrangement of two linear dimers (a), pinwheel structure (b), cyclic structure (c).

TABLE 14: Computed MP2 Equilibrium Structures of Different Cyanoacetylene Tetramers[a]

	basis set			basis set	
	I	II		I	II
			Linear		
r(H−C)	1.0647	1.0633	r(H−C)	1.0714	1.0697
r(C≡C)	1.2235	1.2118	r(C≡C)	1.2252	1.2135
r(C−C)	1.3752	1.3685	r(C−C)	1.3740	1.3675
r(C≡N)	1.1857	1.1739	r(C≡N)	1.1862	1.1743
r(N- - -H)	2.2123	2.2518	r(N- - -H)	2.2153	2.2564
r(H−C)	1.0707	1.0691	r(H−C)	1.0704	1.0689
r(C≡C)	1.2251	1.2133	r(C≡C)	1.2251	1.2134
r(C−C)	1.3739	1.3675	r(C−C)	1.3760	1.3694
r(C≡N)	1.1860	1.1741	r(C≡N)	1.1879	1.1753
r(N- - -H)	2.1923	2.2321			
			Antiparallel Stacked		
r(H−C)	1.0653	1.0639	∠(H−C≡C)	177.5	178.9
r(C≡C)	1.2244	1.2126	∠(C≡C−C)	179.5	178.3
r(C−C)	1.3741	1.3673	∠(C−C≡N)	179.5	179.4
r(C≡N)	1.1860	1.1742	∠(C≡N- - -H)	176.6	177.4
r(N- - -H)	2.1953	2.2283	∠(N- - -H−C)	177.5	178.1
r(H−C)	1.0712	1.0697	∠(H−C≡C)	179.9	179.1
r(C≡C)	1.2259	1.2142	∠(C≡C−C)	178.5	177.1
r(C−C)	1.3746	1.3679	∠(C−C≡N)	178.1	177.7
r(C≡N)	1.1881	1.1757	∠(C≡N- - -H′)	95.4	95.3
r(N- - -H′)	3.0003	3.0468	∠(N- - -H′−C′)	97.4	96.9
			Cyclic		
r(H−C)	1.0691	1.0676	∠(H−C≡C)	177.3	177.7
r(C≡C)	1.2250	1.2132	∠(C≡C−C)	178.7	178.4
r(C−C)	1.3678	1.3678	∠(C−C≡N)	178.9	178.4
r(C≡N)	1.1873	1.1749	∠(C≡N- - -H′)	131.3	131.4
r(N- - -H)	2.3052	2.3077	∠(N- - -H′−C′)	143.9	144.1
			Pinwheel		
r(H−C)	1.0663	1.0645	$r(\pi)^b$	2.59	2.56
r(C≡C)	1.2251	1.2132	∠(H−C≡C)	179.0	179.0
r(C−C)	1.3773	1.3701	∠(C≡C−C)	179.5	178.6
r(C≡N)	1.1880	1.1755	∠(C−C≡N)	179.5	179.0

[a] Distances are given in angstroms and angles in degrees. [b] Distance from H to the center of the C≡C triple bond, π-type hydrogen bond length.

TABLE 15: Computed MP2 Stabilization Energies (ΔE), BSSE-Corrected Stabilization Energies (ΔE(BSSE)), and ZPE-Corrected Stabilization Energies (ΔE(ZPE)) for Linear $C_{\infty v}$, Stacked Antiparallel, C_{2h}, Cyclic, C_{4h}, and Pinwheel, C_{4h}, Cyanoacetylene Tetramers (kcal mol^{-1})

	linear basis set		antiparallel stacked[a] basis set		cyclic[b] basis set		pinwheel[c] basis set	
	I	II	I	II	I	II	I	II
ΔE	−16.21	−14.20	−17.39	−16.37	−17.29	−15.50	−5.45	−4.07
BSSE	2.75	1.15	4.89	3.93	3.22	2.02	3.95	4.14
ΔE(BSSE)	−13.46	−13.05	−12.50	−12.44	−14.07	−13.48	−1.50	+0.07
ZPE	2.49		2.15		1.68		2.18	
ΔE(ZPE)	−13.72	−11.71[d]	−15.24	−14.22[d]	−15.41	−13.82[d]	−3.27	−1.89[d]
ΔE(BSSE + ZPE)	−10.97	−10.56	−10.35	−10.29	−12.19	−11.80	+0.72	+2.25

[a] See Figure 6a. [b] See Figure 6c. [c] See Figure 6b. [d] ZPE corrections taken from basis set I results.

TABLE 16: Computed MP2 C−H Stretching and CCH Bending Frequencies, Frequency Shifts Relative to the Monomer, and Infrared Intensities for Four Different Cyanoacetylene Tetramer Structures As Obtained with Basis Set I[a]

linear	antiparallel stacked	cyclic	pinwheel
	C−H Stretching Frequencies		
3525 (*−6*) [88]	3519 (*−12*) [0]	3469 (*−62*) [0]	3502 (*−29*) [0]
3445 (*−86*) [381]	3519 (*−12*) [173]	3467 (*−64*) [930]	3500 (*−31*) [886]
3443 (*−88*) [280]	3436 (*−95*) [1057]	3464 (*−67*) [0]	3494 (*−37*) [0]
3432 (*−99*) [1170]	3433 (*−98*) [0]		
	CCH Bending Frequencies		
799 (*189*) [57]	798 (*188*) [68]	702 (*92*) [153]	750 (*140*) [0]
790 (*180*) [81]	796 (*186*) [0]	702 (*92*) [0]	726 (*116*) [130]
784 (*176*) [79]	773 (*163*) [0]	702 (*92*) [0]	725 (*115*) [131]
621 (*11*) [93]	769 (*159*) [80]	675 (*65*) [0]	710 (*100*) [0]
	643 (*33*) [84]	674 (*64*) [394]	708 (*98*) [0]
	642 (*32*) [0]	672 (*62*) [0]	699 (*89*) [0]
	609 (*−1*) [127]		
	609 (*−1*) [0]		

[a] Frequencies and shifts relative to the monomer (in italics and in parentheses) in cm^{-1}, infrared intensities in square brackets in km mol^{-1}.

Compared to the antiparallel dimer (3.2−3.3 Å), the antiparallel stacked tetramer shows a much smaller intermolecular *outer (stacking) hydrogen-bond distance* of about 3.0−3.05 Å, if one is willing to accept the C−H- - -N≡C arrangement with ∠C−H- - -N and ∠H- - -N≡C bond angles close to 90° as a conventional hydrogen bond at all. Compared to the linear dimer, the *inner* hydrogen bonds are further contracted in the antiparallel stacked tetramer. In this tetramer, the two antiparallel dimers are banana-shaped, thus displaying a significantly larger intermolecular distance in the center (about 3.7 Å).

The computed pinwheel structure has very long π-type hydrogen bonds of about 2.6 Å, very similar to the case of the π-type hydrogen-bonded dimer (see the contour map in Figure 2). Optimization attempts within the framework of SCF and B3LYP approaches, when starting from MP2-optimized structures for the antiparallel stacked tetramer or the pinwheel tetramer, all invariably ended up at the cyclic C_{4h} structure. This is fully compatible with the behavior already observed when investigating the dimer energy surface. The stacked arrangements are not properly described at the SCF and B3LYP levels, and the π-type hydrogen bond is inherently weak.

From the four structures considered, the pinwheel arrangement is by far the least stable. Actually, it is barely bound, even at the MP2 level. At least with basis sets I and II, the bare total interaction energy of the pinwheel tetramer with four π-type hydrogen bonds is similar in magnitude to that of the single hydrogen bond in the linear dimer. Upon correcting for ZPE and BSSE, the latter being very questionable with basis set I as already discussed before, the pinwheel structure is even repulsive. Hence, it is not a good candidate for an experimentally observable complex. From the computed interaction energies, the other three structures are all of comparable stability. With the MP2 data, as obtained with basis sets I and II, the cyclic C_{4h} configuration is about 1−2 kcal mol^{-1} more stable than the other two. From the experience gained with the larger basis-set calculations on the trimers and in particular on the dimers, one can extrapolate that upon further improving the quality of the calculations, the relative stabilities are probably shifted most strongly in favor of the antiparallel stacked tetramer and least in the direction of the linear structure.

Turning to the computed frequency shifts, we note that the antiparallel stacked tetramer behaves like a weakly coupled pair of linear dimers, however, with somewhat stronger red-shifted C−H stretching bands, in line with the somewhat contracted intermolecular hydrogen-bond distance (about 0.05 Å shorter than in the linear dimer and about 0.03 Å shorter than in the linear trimer). Two infrared-active C−H stretching frequencies are predicted for that structure, with an intensity ratio of about 1:6 and shifts of −12 and −95 cm^{-1}, respectively. The first one originates from the C−H stretchings in the *outer hydrogen bonds* and the latter from the *inner* hydrogen-bonded C−H groups. From the three close-lying C−H stretches of the cyclic C_{4h} tetramer, only one (doubly degenerate) is infrared active with a computed shift of −64 cm^{-1}. For the linear tetramer, the computed infrared intensity ratio between the most intense and the next two intense bands is on the order of 3−4, implying that when the most intense band is observed, then, most probably, the other two should be visible as well. For the pinwheel structure, a single infrared-active C−H stretching mode is predicted with a shift of −31 cm^{-1}, close to the C−H stretching mode of the cyclic trimer. However, as discussed before, the pinwheel structure can be excluded on energetic grounds. Generally, the splitting and intensity patterns of the CCH bending frequencies reported in Table 16 suggest that, again, an investigation of this spectral region could be very useful for the assignment problem.

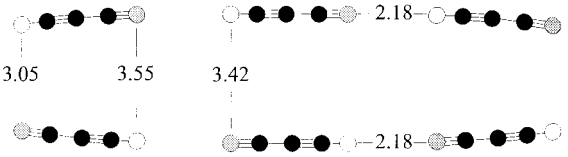

Figure 7. Structure of the antiparallel stacked cyanoacetylene hexamer.

TABLE 17: Computed MP2 (Basis Set I) Stabilization Energies (ΔE) and BSSE-Corrected Stabilization Energies (ΔE(BSSE)) for Linear, $C_{\infty v}$, and Cyclic, C_{5h}, Cyanoacetylene Pentamers and Linear $C_{\infty v}$, Cyclic, C_{6h}, and Antiparallel Stacked, C_{2h}, Cyanoacetylene Hexamers (kcal mol^{-1})

	linear	cyclic	antiparallel stacked
		Pentamers	
ΔE	−22.00	−23.95	
BSSE	3.70	4.05	
ΔE(BSSE)	−18.30	−19.90	
		Hexamers	
ΔE	−27.82	−30.45	−31.41
BSSE	4.65	4.95	8.42
ΔE(BSSE)	−23.17	−25.50	−22.99

Attempts have also been undertaken to model the energy surface for the transition from the cyclic C_{4h} structure to the antiparallel stacked C_{2h} configuration. However, from preliminary calculations, it was soon realized that at the current stage this is too ambitious of a goal. Too many soft degrees of freedom are involved in this process, and the definition of a reasonable *reaction path* without foregoing extensive scans of the high-dimensional energy surface is not possible. Hence, this goal has been given up for the time being.

E. Pentamer and Hexamer. The computed C−H bond distances and intermolecular H- - -N distances of linear and cyclic hexamers obtained at the basis set I MP2 level were already reported in ref 15. In addition to these calculations, an antiparallel stacked hexamer structure has been treated consisting of a pair of linear trimers. For a sketch of the optimized structure, see Figure 7. One can observe the following trends: (i) the local structure of the *outer hydrogen bonds* of the antiparallel stacked hexamer is very similar to that in the antiparallel stacked tetramer; (ii) the two *inner* hydrogen bonds are about equal, as they were in the isolated linear trimers, however, they are now shorter by 0.04 Å; (iii) the intermolecular distances between the centers of the two trimers or the two hydrogen bonds in the trimers are distinctly smaller than the corresponding geometric parameters in the stacked antiparallel tetramer. The demands of the MP2 vibrational analyses surpassed our computing resources. Hence, in Table 17, only the computed stabilization energies and the corresponding BSSE-corrected values are reported. For pentamers and hexamers, with and without BSSE corrections, the cyclic forms are more stable than the linear clusters. Taking the uncorrected stabilization energy, the antiparallel stacked hexamer is slightly more stable than the cyclic hexamer. To use the very large BSSE correction in the case of the antiparallel stacked hexamer produces an artifact certainly. From the foregoing experience, it is to be expected that the stacked antiparallel hexamer is the most stable hexamer.

F. Relation to Experiment. In their experimental investigation of the C−H-stretching region of cyanoacetylene clusters, Yang et al.[2] observed at least 12 distinct bands (see Table 3 of ref 2). Their band labeled 1 with a red shift of −3 cm^{-1} corresponds, undoubtedly, to the stretching motions of the non-hydrogen-bonded, *free* C−H groups of the linear dimer and the linear trimer for which we calculated shifts of −2 to −5 cm^{-1}. For the linear dimer, the experimental red shift of −66.5 cm^{-1} (band labeled 6) also compares well to the calculated shifts of −72, −67, and −78 cm^{-1} with basis sets I−III. From all the remaining experimental bands, only one originates from a polar species, as revealed from measurements in large electric fields. This band labeled as 8 with a shift of −80.5 cm^{-1} has been assigned to the in-phase stretch combination of the two hydrogen-bonded C−H groups of the linear trimer. For this mode of the linear trimer, we computed shifts of −92 (basis set I) and −80 cm^{-1} (basis set II), in good agreement with the experimental value. The band labeled 3 with an experimental red shift of −33 cm^{-1} was assigned to the cyclic trimer. For that we obtain (basis set I) a computed shift of −33 cm^{-1}, thus confirming the assignment of Yang et al. The remaining eight bands all must originate from nonpolar structures and must originate from clusters at least of the size of tetramers. Of particular interest is the band labeled 2 with a shift of about −12 cm^{-1}. Because of the small shift, it must stem from a structure in which the C−H group is only very weakly distorted. Yang et al. suggested that this band might originate from the pinwheel tetramer. On the basis of the calculations just discussed, we can exclude that. However, the calculated shifts for the case of the antiparallel stacked tetramer suggest that this band corresponds to a C−H stretch in the *outer hydrogen bond* of that cluster (computed shift −12 cm^{-1}) and that it must always appear together with a much stronger shifted and significantly more intense band (−95 cm^{-1}). This computed shift could fit to the band labeled as 9 (shift −93 cm^{-1}).[45] This is confirmed by the fact that bands 2 and 9 suffer, as reported in ref 2, very similar intensity losses when the source is heated from 295 to 350 K. Moreover, it is to be expected that the antiparallel stacked hexamer, for which the theoretical vibrational analysis could not be done, also has one band close to the one shifted by −12 cm^{-1}, since the local geometry of the *outer* C−H- - -N moiety is already very similar to that in the antiparallel stacked tetramer. Again, at least one or two stronger-shifted bands, eventually labeled as 10 and/or 11 with experimental shifts of −102 and −107 cm^{-1}, which originate from the C−H stretches in the *inner* hydrogen bonds, must also appear. Furthermore, it is interesting to note that the source pressure dependence of the intensity of band 2 has an unusual behavior which is consistent with the notion that its intensity may be due to more than one species.

So far, the bands labeled as 4, 5, and 7 with shifts of −55.5, −62.5, and −78 cm^{-1}, respectively, have not yet been discussed. Most probably and admittedly because of the lack of alternatives, these originate from the cyclic tetramer, pentamer, and hexamer, although our computed shift of −64 cm^{-1} for the tetramer would instead point to band 5 as that of the cyclic tetramer. However, with such small differences, the precise assignment is very difficult from a theoretical aspect.

From infrared[46−48] and Raman[48,49] experiments on solid cyanoacetylene, it is known that the C−H stretching modes in the extended linear hydrogen-bonded chains[50] are found to be shifted by −123 and −118 cm^{-1}, respectively, relative to the monomer. It is to be expected that none of the smaller clusters treated in this work and measured in the gas phase should display larger red shifts in the C−H stretching region.

Summary and Conclusions

A systematic study on the structure and vibrational spectroscopy of chainlike, ring-like, and stacked cyanoacetylene clusters has been presented. One outcome of this investigation is that apart from the linear hydrogen-bonded dimer, a second configuration, the antiparallel stacked dimer, is also a distinct

minimum on the energy surface and that its stabilization energy is actually very close to that of the linear dimer. Hence, it should be experimentally observable. So far, this type of dimeric complex has not yet been detected. A second outcome of this investigation is that a C_{2h}-symmetric tetramer built from an antiparallel arrangement of linear dimers is a minimum on the energy surface with a stability close to or even greater than that of the C_{4h} ring structure. Similarly, a stacked hexamer built from antiparallel linear trimers is probably already more stable than the C_{6h} ring. From the tetramers on, the linear clusters are energetically disfavored compared to their cyclic or stacked counterparts. This is in agreement with the experimental findings.[2] The largest polar cluster that could be experimentally detected corresponded to the linear trimer. It appears that solidlike clusters which are stabilized by hydrogen bonding within short chains and electrostatic and dispersion interactions between these short chains are already the dominant species for comparatively small cluster sizes.

The theoretical vibrational analysis performed allowed for an almost complete assignment of the experimentally observed C−H-stretching modes. The complete vibrational analysis also showed that apart from the C−H-stretching region, the region of the CCH-bending modes (660−750 cm^{-1}) appears most promising for gaining additional information to help in the assignment problem and in the identification of the clusters present in the vapor phase. It is well-known[47,48] that from the monomer (663 cm^{-1}) to the crystal (749 cm^{-1}), a blue shift of 86 cm^{-1} takes place for the CCH-bending mode. The calculations demonstrated that sufficiently different blue shifts can be expected for the various cluster types. Because of the somewhat bent cyanoacetylene monomers in the cyclic and stacked clusters, it may even be the case that some of the cluster blue shifts exceed the crystal blue shift. Only very small shifts can be expected for the other intramolecular stretching and bending modes of cyanoacetylene upon increasing the cluster size.

From the methodical side, the calculations have, not surprisingly, demonstrated that neither the SCF nor the DFT approach is useful when structures have to be compared in which either electrostatic or dispersion contributions are dominating. Moreover, the calculations have also shown that great care must be applied when one wishes to improve medium basis-set results by naively using the counterpoise procedure. For the case in hand, it rather appears preferable to use the uncorrected interaction energies. When basis sets are used which are sufficiently large to give reasonable anisotropic polarizabilities (basis set III), the BSSE corrections are significantly smaller, although clearly not negligible. Application of the BSSE correction in cases where the errors in the polarizability already cause a significant underestimation of the interaction energy results in an increase of the error rather than in an improvement.

Acknowledgment. The calculations were performed on the Cluster of Digital Alpha Servers (2100 4/275 and 5/375) of the computer center of the University of Vienna and on local RISC 6000/550 and Silicon Graphics workstations at the Institute of Theoretical Chemistry and Radiation Chemistry of the University of Vienna. The author is grateful for ample supply of computer time on these installations.

References and Notes

(1) Kerstel, E. R. Th.; Scoles, G.; Yang, X. *J. Chem. Phys.* **1993**, *99*, 876.

(2) Yang, X.; Kerstel, E. R. Th.; Scoles, G.; Bemish, R. J.; Miller, R. E. *J. Chem. Phys.* **1995**, *103*, 8828.

(3) Maroncelli, M.; Hopkins, G. A.; Nibler, J. W.; Dyke, Th. R. *J. Chem. Phys.* **1988**, *88*, 2196.

(4) Hopkins, G. A.; Maroncelli, M.; Nibler, J. W.; Dyke, Th. R. *Chem. Phys. Lett.* **1985**, *114*, 97.

(5) Anex, D. S.; Davidson, E. R.; Douketis, C.; Ewing, G. E. *J. Phys. Chem.* **1988**, *92*, 2913.

(6) Jucks, K. W.; Miller, R. E. *J. Chem. Phys.* **1988**, *88*, 2196.

(7) Jucks, K. W.; Miller, R. E. *J. Chem. Phys.* **1988**, *88*, 6059.

(8) Miller, R. E. *Science* **1988**, *240*, 447.

(9) Ruoff, R. S.; Emilsson, T.; Klots, T. D.; Chuang, C.; Gutowsky, H. S. *J. Chem. Phys.* **1988**, *89*, 138.

(10) Meyer, H.; Kerstel, E. R. Th.; Zhuang, D.; Scoles, G. *J. Chem. Phys.* **1989**, *90*, 4623.

(11) Kerstel, E. R. Th.; Lehmann, K. K.; Gambogi, J. E.; Yang, X.; Scoles, G. *J. Chem. Phys.* **1993**, *99*, 8559.

(12) Tostes, J. G. R.; Taft, C. A.; Ramos, M. N. *J. Phys. Chem.* **1987**, *91*, 3157.

(13) Taft, C. A.; Azevedo, J. C.; Tostes, J. G. R.; Lester, W. A., jr. *J. Mol. Struct.* (*THEOCHEM*) **1988**, *168*, 169.

(14) Platts, J. A.; Howard, S. T.; Fallis, I. A. *Chem. Phys. Lett.* **1998**, *285*, 198.

(15) Karpfen, A. *J. Phys. Chem.* **1996**, *100*, 13474.

(16) Frisch, M. J.; Trucks, G. W.; Schlegel, H. B.; Gill, P. M. W.; Johnson, B. G.; Robb, M. A.; Cheeseman, J. R.; Keith, T. A.; Petersson, G. A.; Montgomery, J. A.; Raghavachari, K.; Al-Laham, M. A.; Zakrzewski, V. G.; Ortiz, J. V.; Foresman, J. B.; Cioslowski, J.; Stefanov, B. B.; Nanayakkara, A.; Challacombe, M.; Peng, C. Y.; Ayala, P. Y.; Chen, W.; Wong, M. W.; Andres, J. L.; Replogle, E. S.; Gomperts, R.; Martin, R. L.; Fox, D. J.; Binkley, J. S.; Defrees, D. J.; Baker, J.; Stewart, J. J. P.; Head-Gordon, M.; Gonzalez, C.; Pople, J. A. *Gaussian 94*, Revision C.2; Gaussian, Inc.: Pittsburgh, PA, 1995.

(17) Møller, C.; Plesset, M. S. *Phys. Rev.* **1934**, *46*, 618.

(18) Becke, A. D. *Phys. Rev.* **1988**, *A38*, 3098.

(19) Becke, A. D. *J. Chem. Phys.* **1993**, *98*, 5648.

(20) Lee, C.; Yang, W.; Parr, R. G. *Phys. Rev.* **1988**, *B37*, 785.

(21) Mielich, B.; Savin, A.; Stoll, H.; Preuss, H. *Chem. Phys. Lett.* **1989**, *157*, 200.

(22) Kofranek, M.; Karpfen, A.; Lischka, H. *Chem. Phys.* **1987**, *113*, 53.

(23) Kofranek, M.; Lischka, H.; Karpfen, A. *Mol. Phys.* **1987**, *61*, 1519.

(24) Kurnig, I. J.; Lischka, H.; Karpfen, A. *J. Chem. Phys.* **1990**, *92*, 2469.

(25) Hehre, W. J.; Ditchfield, R.; Pople, J. A. *J. Chem. Phys.* **1972**, *56*, 2257.

(26) Frisch, M. J.; Pople, J. A.; Binkley, J. S. *J. Chem. Phys.* **1984**, *80*, 3265.

(27) Huzinaga, S. *J. Chem. Phys.* **1965**, *42*, 1293.

(28) Huzinaga, S. *Approximate Atomic Functions I*; University of Alberta: Edmonton, Canada, 1971.

(29) Krishnan, R.; Binkley, J. S.; Seeger, R.; Pople, J. A. *J. Chem. Phys.* **1980**, *72*, 5639.

(30) Clark, T.; Chandrasekhar, J.; Spitznagel, G. W.; Schleyer, P. v. R. *J. Comput. Chem.* **1983**, *4*, 294.

(31) Boys, S. F.; Bernardi, F. *Mol. Phys.* **1970**, *19*, 553.

(32) Botschwina, P.; Horn, M.; Seeger, S.; Flügge, J. *Mol. Phys.* **1993**, *78*, 191.

(33) Mallinson, P. D.; de Zafra, R. L. *Mol. Phys.* **1978**, *36*, 827.

(34) Arnau, A.; Silla, E.; Tunon, I. *Astrophys. J.* **1993**, *415*, L151.

(35) Francisco, J. S.; Richardson, S. L. *J. Chem. Phys.* **1994**, *101*, 7707.

(36) Hu, Ch.; Schaefer, H. F., III *J. Phys. Chem.* **1993**, *97*, 10681.

(37) Lee, S. *J. Mol. Struct.* (*THEOCHEM*), **1998**, *427*, 267.

(38) Lafferty, W. J.; Lovas, F. J. *J. Phys. Chem. Ref. Data* **1978**, *7*, 441.

(39) Fowler, P. W.; Diercksen, G. H. F. *Chem. Phys. Lett.* **1990**, *167*, 105.

(40) Mallinson, P. D.; Fayt, A. *Mol. Phys.* **1976**, *32*, 473.

(41) Yamada, K. M. T.; Moravec, A.; Niedenhoff, M.; Bürger, H.; Winnewisser, G. *Z. Naturforsch.* **1996**, *51a*, 27.

(42) Simandiras, E. D.; Rice, J. E.; Lee, T. J.; Amos, R. D.; Handy, N. C. *J. Chem. Phys.* **1988**, *88*, 3187.

(43) Kristyan, S.; Pulay, P. *Chem. Phys. Lett.* **1994**, *229*, 175.

(44) Proynov, E. I.; Ruiz, E.; Vela, A.; Salahub, D. R. *Int. J. Quantum Chem. Symp.* **1995**, *29*, 61.

(45) Scoles, G. private communication.

(46) Turrell, G. C.; Jones, W. D.; Maki, A. *J. Chem. Phys.* **1957**, *26*, 1544.

(47) Uyemura, M.; Maeda, S. *Bull. Chem. Soc. Jpn.* **1974**, *47*, 2930.

(48) Nolin, C.; Weber, J.; Savoie, R. *J. Raman Spectrosc.* **1976**, *5*, 21.

(49) Aoki, K.; Kakudate, Y.; Yoshida, M.; Usuba, S.; Fujiwara, S. *J. Chem. Phys.* **1989**, *91*, 2814.

(50) Shallcross, F. V.; Carpenter, G. B. *Acta Crystallogr.* **1958**, *11*, 490.